JOURNAL OF SOLID STATE CHEMISTRY 59, 190–200 (1985)

Study of Copper-Chromium Oxide Catalyst

I. Thermal Decomposition of Copper(II) Chromate, $CuCrO_4$*

F. HANIC, I. HORVÁTH, G. PLESCH, AND Ľ. GÁLIKOVÁ

Institute of Inorganic Chemistry, Chemical Research Centre, Slovak Academy of Sciences, 84236 Bratislava, Dúbravská cesta, Czechoslovakia

Received September 6, 1984

The kinetics, mechanism, and activation energy of the isothermal decomposition of $CuCrO_4$ was studied using an isothermal TG method and an X-ray high-temperature diffraction technique in either air or a flowing atmosphere of N_2. The enthalpy change ΔH of the decomposition reaction

$$2CuCrO_4 \rightarrow CuO + CuCr_2O_4 + \tfrac{3}{2}O_2$$

was determined by DSC analysis. The mechanism of the thermal decomposition of $CuCrO_4$ is well represented by the standard Avrami–Erofeev kinetic equation $[-\ln(1 - \alpha)]^{1/2} = kt$. According to this mechanism, the reaction rate is controlled by the formation and growth of nuclei on the surface of the reactant. The activation energy E_A of the process in air is $E_A = (248 \pm 8)$ kJ mole^{-1}, in flowing atmosphere of nitrogen $E_A = (229 \pm 8)$ kJ mole^{-1}. ΔH in air is 110 kJ mole^{-1}, in flowing nitrogen 67 kJ mole^{-1}. The lower values of ΔH and E_A in the flowing atmosphere of nitrogen are due to the fast elimination of O_2 from the reaction interface. However, the decay of the crystalline portion of $CuCrO_4$ during its thermal decomposition, studied by the X-ray diffraction, is controlled by a different reaction mechanism (first-order kinetics). The reaction mechanism is discussed in the relation to the crystal structure of the reactants.

1. Introduction

The catalytic activity and selectivity of the system $CuO + CuCr_2O_4$, well known as Adkins' catalyst (*1–3*), vary with the method of preparation and the conditions of the pretreatment (*4*). They depend on the crystallinity of present phases (crystallite size (*5*), portion of the amorphous phases), on the oxidation state of ions as well as on the occurrence of defects, on the distribution of the transition metal ions over the tetrahedral and octahedral sites in the spinel-like $CuCr_2O_4$ structure, on the nature of support, and on the presence of the vacancies and the reaction conditions. The system is active in several oxidation, hydrogenation, dehydrogenation, alkylation, etc. (*1, 2, 4*) reactions.

The preparation of the catalyst by autocatalytic thermal decomposition of the $Cu(OH)(NH_4)CrO_4$ complex occurs according to the reaction (*1, 5*)

$$2Cu(OH)(NH_4)CrO_4 \xrightarrow{573\text{–}773\ K} CuO(s) + CuCr_2O_4(s) + N_2(g) + 5H_2O(g) \quad (1)$$

At higher temperatures, a reduction of

---

* Dedicated to the 60th birthday of Professor J. J. Dunitz.

0022-4596/85 $3.00

Cu(II) to Cu(I) proceeds according to the reaction (*6*)

$$CuO + CuCr_2O_4 \xrightarrow[1098\text{–}1173\ \text{K in air}]{1013\text{–}1078\ \text{K in nitrogen}} 2CuCrO_2 + \tfrac{3}{2}O_2 \quad (2)$$

The catalytic system $CuO + CuCr_2O_4$ can be obtained by thermal decomposition of coprecipitated copper and chromium hydroxides (hydroxynitrates) (*7, 8*).

The direct solid-state reaction between CuO and Cr_2O_3 takes place at higher temperatures (above 970 K) (*9, 10*).

In this paper is studied the isothermal decomposition of $CuCrO_4$ by a thermogravimetric (TG) method and X-ray analysis according to the reaction (*10*)

$$2CuCrO_4 \xrightarrow{687\text{–}773\ \text{K}} CuO + CuCr_2O_4 + 1.5\ O_2 \quad (3)$$

primarily to determine the kinetics, mechanism, activation energy E_A, and enthalpy change ΔH of the decomposition in air and inert atmosphere. Reaction (3) seems to be better applicable for the interpretation of the reduction process $Cr^{6+} \rightarrow Cr^{3+}$, since the thermal decomposition of copper chromate below 800 K proceeds in one step only (*10*), in contradistinction to the two-step reaction (1) (*11*).

2. Experimental

Copper chromate was obtained by the mixing of aqueous solutions of $Cu(NO_3)_2$ and $(NH_4)_2Cr_2O_7$, both of analytical quality, according to

$$2Cu^{2+} + (Cr_2O_7)^{2-} + 2(OH)^- \rightarrow 2CuCrO_4 + H_2O \quad (4)$$

The solutions were evaporated to dryness. The precursor thus obtained was heated at 473–523 K in air for 4 h, in order to eliminate the volatile components and to decompose the nitrate. The phase purity of the powder sample was checked by X-ray diffraction comparing its powder diffraction pattern with a standard pattern of $CuCrO_4$ (*18*) and by weight loss during heating corresponding to reaction (3).

Thermal decomposition of $CuCrO_4$ according to reaction (3) was studied using a DuPont Thermoanalyzer (TGA 951 and DSC modules). The weight losses during isothermal decomposition of powder samples (15–20 mg) were measured (a) in air and (b) in a flowing atmosphere of N_2 (flow rate: 1 $cm^3\ s^{-1}$).

DSC analysis of the enthalpy change ΔH of reaction (3) was performed with samples of 5–7 mg. The calibration coefficient k in the formula for the calculation of ΔH

$$\Delta H = kAm^{-1}$$

was found by means of the measurements performed with standard materials (In, Sn, Zn, K_2SO_4, SiO_2) in the temperature interval 420–850 K. A and m represent DSC peak area and the mass of the sample, respectively.

The rate of the $CuCrO_4$ decomposition, according to reaction (3), was checked by the high-temperature X-ray powder diffraction method in static air. The changes of the integral intensities of the selected reflections *hkl* corresponding to the dissociating crystalline $CuCrO_4$ were evaluated as a function of time t at different temperature levels. The fraction decomposed α vs t was evaluated from the relation

$$\alpha = 1 - \frac{I(t)}{I_0},$$

where $I(t)$ is the integral intensity I_{hkl} of $CuCrO_4$ in time t and I_0 is the integral intensity I_{hkl} of the same reflection at the beginning of the reaction. $I(t)$ were evaluated from the line profile analysis as well as from the continuous peak intensity decrease as a function of time t. The measurements were performed on a Rigaku–Denki high-temperature powder diffraction device, using Cu*K*α radiation. During isothermal experiments, the temperature was stable within ±2 K.

The electronic spectra of solids were recorded on a Specord UV-VIS spectrometer (C. Zeiss, Jena) in Nujol mulls in the range 12,500–30,000 cm^{-1}.

3. Results and Discussion

The kinetics of the isothermal decomposition of copper chromate were studied thermogravimetrically at the following temperatures: in air at 713.5, 733, 743, 747, and 756 K; in a flowing atmosphere of N_2 at 687, 709.5, 721, and 729 K. Fractions decomposed (α) were calculated from the isothermal weight losses in time t divided by the theoretical total weight loss of reaction (3): 13.37% O (found: 13.30% O).

The plots of α vs t are shown in Fig. 1 (decomposition in air) and in Fig. 2 (decomposition in a flowing atmosphere of N_2). All curves exhibite typical induction, acceleratory and decay periods. Transformation of these curves from the type $\alpha = f(t)$ into a form $\alpha = f(t/t_{0.5})$, where $t_{0.5}$ represents the time for 50% of the completion, gives the distribution of the experimental points along a typical curve (Fig. 3). The experimental points in Fig. 3 come from transformed isotherms measured in air at 743 and 756 K and in a flowing inert atmosphere at 687 and 721 K. Distribution of all experimental points over the range α = 0.2–0.9 obeys the form of the model curve represented by Avrami–Erofeev kinetic equation derived in different ways (*12–15*):

$$[-\ln(1 - \alpha)]^{1/n} = kt. \tag{6}$$

The value of n in (6) depends on the shape of nuclei, on the number of nuclei present at the beginning of reaction (3), and their distribution in particles. Figure 4 shows plots of $\ln[-\ln(1 - \alpha)]$ vs $\ln t$. Linear

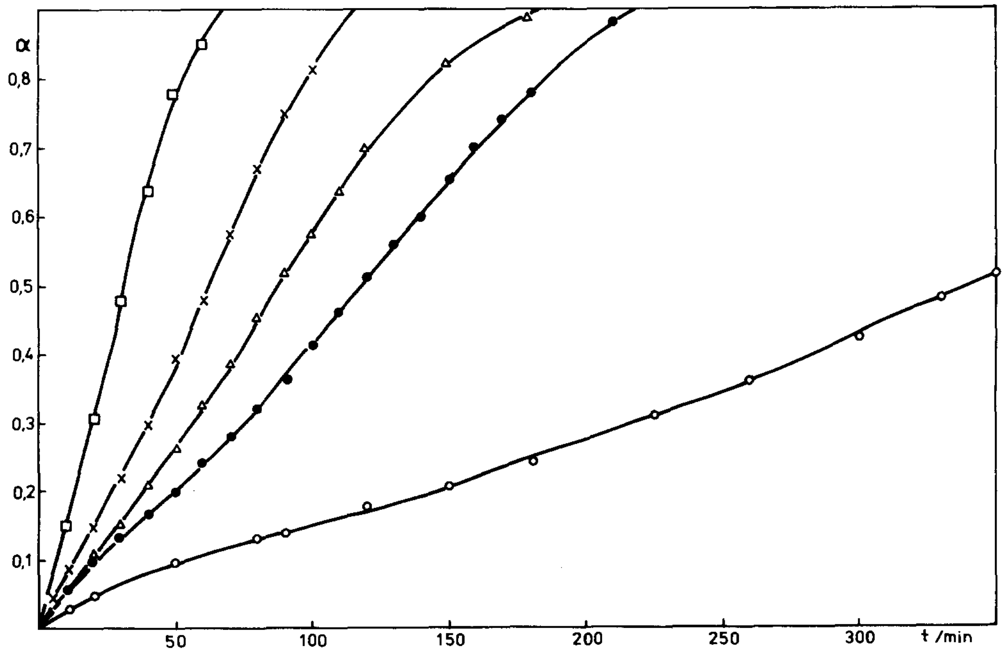

FIG. 1. The plot of α vs t for isothermal decomposition of $CuCrO_4$ in air at 713.5 K (○), 733 K (●), 743 K (△), 747 K (×), 756 K (□).

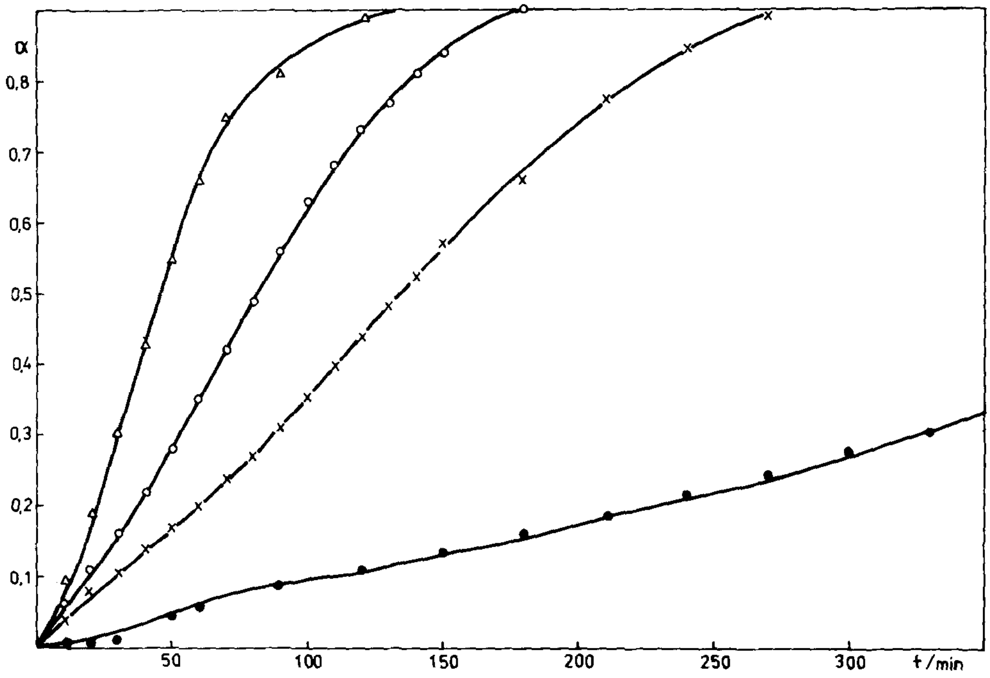

FIG. 2. The plot of α vs t for isothermal decomposition of $CuCrO_4$ in a flowing atmosphere of N_2 (1 $cm^3\ s^{-1}$) at 687 K (●), 709.5 K (×), 721 K (○), 729 K (△).

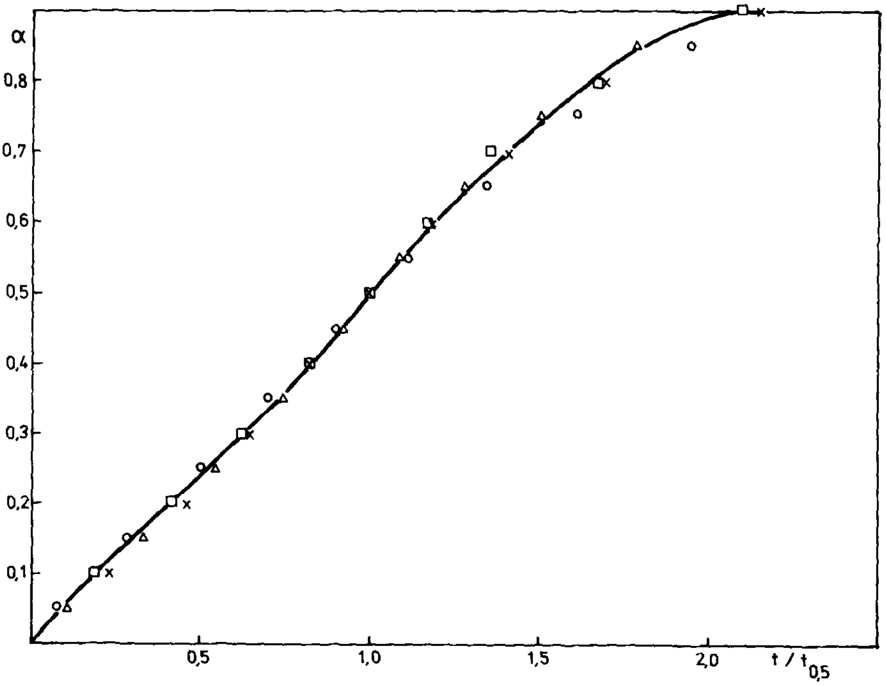

FIG. 3. Transformed isothermal curves of the type $\alpha = f(t/t_{0.5})$, where $t_{0.5}$ is the half-time of the reaction completion. The experimental points come from transformed isotherms measured at 743 and 756 K in air and at 687 and 721 K in a flowing N_2 atmosphere. Distribution of experimental points obeys the form of the model curve represented by the Avrami–Erofeev kinetic equation $[-\ln(1-\alpha)]^{1/n} = kt$ (solid line).

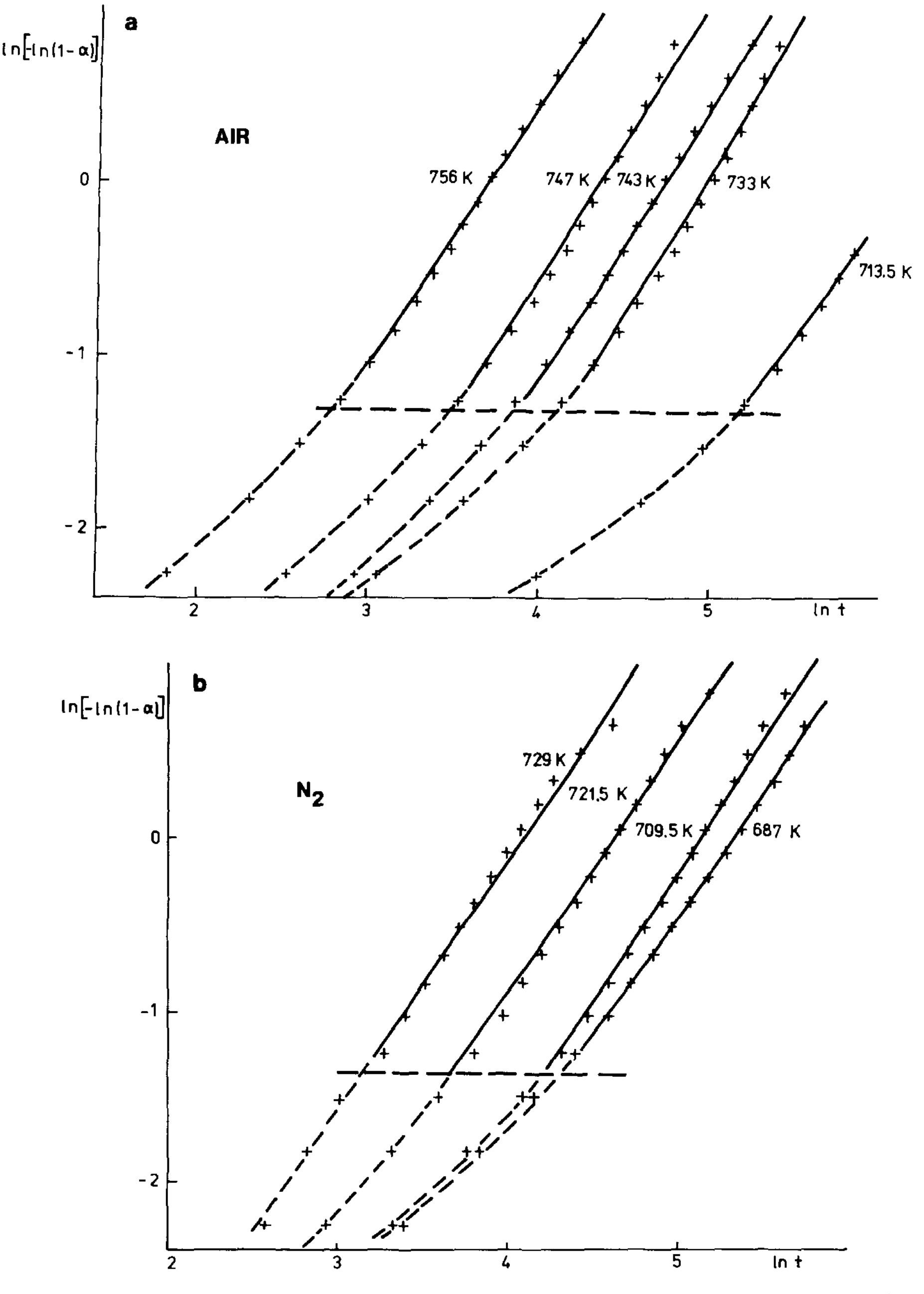

FIG. 4. Plots of ln[−ln(1 − α)] vs ln(t) for isothermal decomposition of $CuCrO_4$ (a) in air and (b) in a flowing N_2 atmosphere. The representative plots are essentially linear for $\alpha = 0.25$–0.9.

dependence with slopes equal to 1.51 ± 0.06 is obtained, indicating that the decomposition of $CuCrO_4$ proceeds through flat nuclei ($n \sim 2$) and the nucleation begins on the surface of each particle. Through the growth of nuclei, at a certain value of α, the overlapping of the product nuclei takes place, and a decrease of the reaction rate

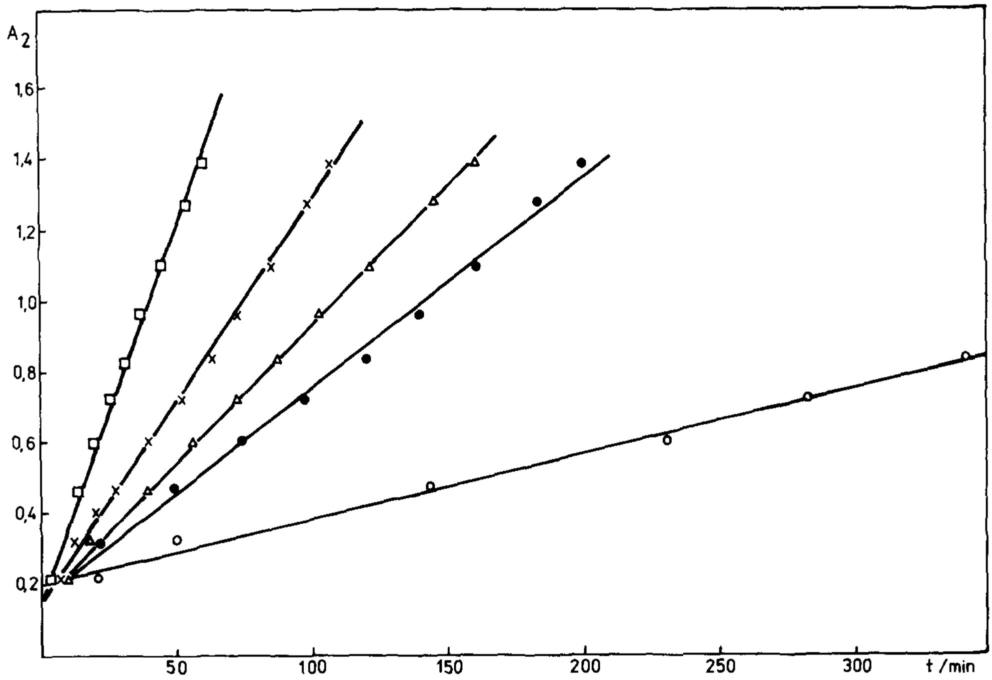

FIG. 5. The representative plot of the isothermal conversions α in air by the Avrami–Erofeev kinetic equation. The designation of temperatures is the same as in Fig. 1.

$d\alpha/dt$ is observed (decay period). The representative plot of the experimental conversions α by equation

$$[-\ln(1 - \alpha)]^{1/2} = kt \qquad (7)$$

is essentially linear both for air (Fig. 5) and for an inert atmosphere (Fig. 6) allowing us to evaluate the temperature coefficients of the rate constants necessary for calculation of the activation energy E_A. While the mechanism of decomposition of $CuCrO_4$ is the same in both atmospheres, the values of the rate constants at corresponding temperatures are greater for the flowing inert atmosphere than for the air due to the easier escape of the gaseous product (O_2) from the phase boundaries of reacting particles in N_2 flow. From the representative Arrhenius plots (Fig. 7) the values of activation energy (E_A) were calculated. $E_A = 248 \pm 8$ kJ mole^{-1} in static air atmosphere and 229 ± 8 kJ mole^{-1} in flowing N_2. The reaction atmosphere significantly influences the values of reaction enthalpies ΔH. In air, $\Delta H = 110$ kJ mole^{-1}, in flowing N_2, $\Delta H = 67$ kJ mole^{-1}.

Copper chromate decomposes on heating with loss of O_2, and the oxidation state of chromium is reduced from +6 to +3 (reaction (3)). Darrie *et al.* (*16*) showed that the activation process for the thermal decomposition of solid chromates is a one-electron transfer from the nonbonding oxygen π-orbital to the chromium ($t_1 \rightarrow 2e$ electronic transition). E_A for the thermal decomposition of chromates may be related to the energy of this charge transfer process; the effect of this is to reduce the oxidation state of chromium from +6 to +5. This rule is well applicable for thermal decomposition of $MgCrO_4$. We found a maximum for $t_1 \rightarrow 2e$ transition at 26,300 cm^{-1} (314.2 kJ mole^{-1}). This energy corresponds well to the activation energy $E_A = 331 \pm 17$ kJ mole^{-1} derived from thermogravimetric studies (*16*). In the case of $CuCrO_4$, a broad absorption can be observed in the short

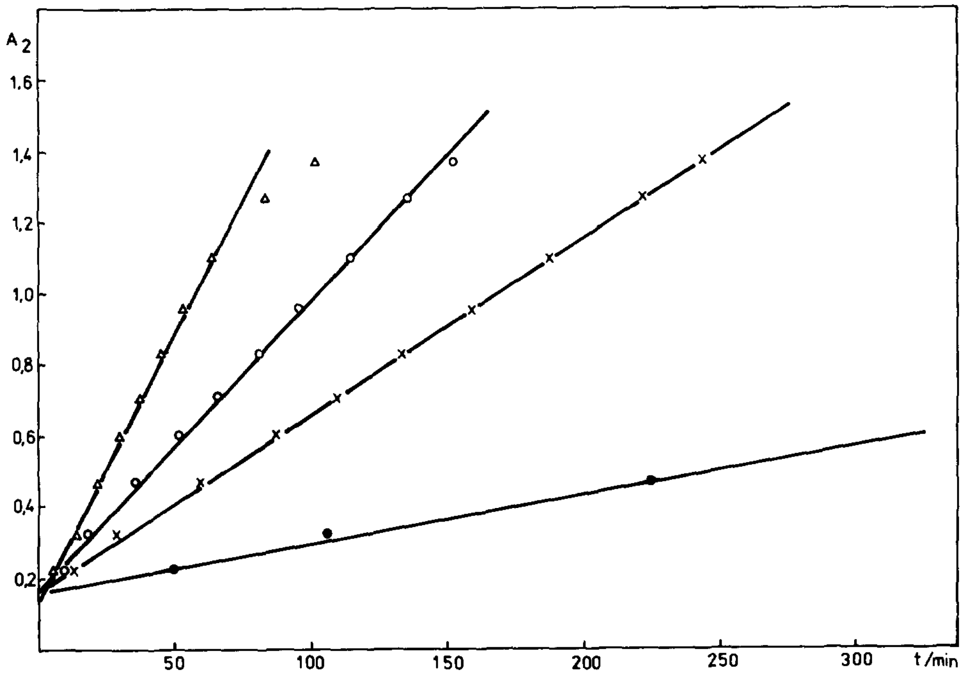

FIG. 6. The representative plot of the isothermal conversions α in a flowing atmosphere of N_2 by the Avrami–Erofeev kinetic equation. The designation of temperatures is the same as in Fig. 2.

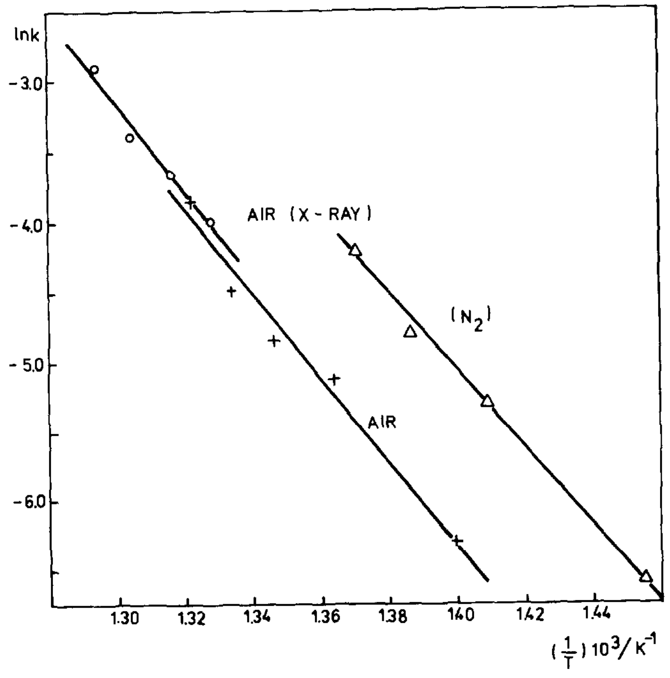

FIG. 7. The representative Arrhenius plots for thermal decomposition of $CuCrO_4$ in air and a flowing atmosphere of N_2.

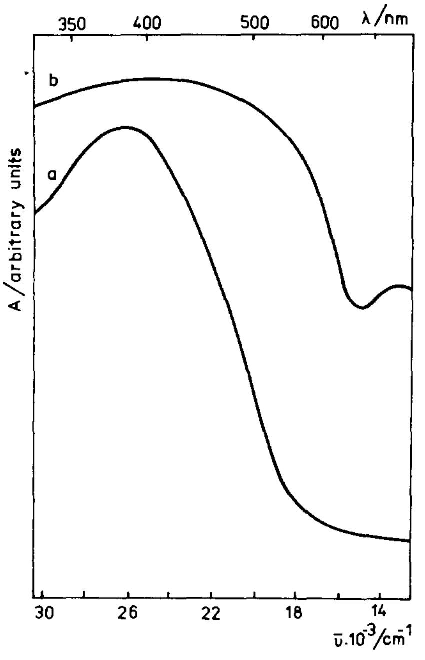

FIG. 8. The electronic spectra of (a) $MgCrO_4$ and (b) $CuCrO_4$.

wavelength side of the visible spectrum (Fig. 8). This absorption band probably consists of charge transfer bands from oxygen to chromium as well as to copper. The weak absorption band at 13,000 cm^{-1} is due to *d–d* transition of Cu^{2+} in octahedral ligand field of oxygen atoms. From such spectrum it is not possible to obtain the precize transfer energy $t_1 \rightarrow 2e$ on CrO_4^{2-} ions. The activation process of chromate decomposition can be propagated according to (*16*), along the rows of CrO_4 tetrahedra with strong anion–anion coupling to the surface where decomposition takes place. The chains of CrO_4 tetrahedra are linked together by the parallel chains of CuO_6 octahedra. Such arrangement is typical for all structures crystallizing in the orthorhombic $CrVO_4$ structure type (*17, 18*). Another important structural feature of the $CrVO_4$ structure type is a strong polarization effect of cations which favor further reduction of Cr^{5+} to Cr^{3+} under formation of the system $CuCr_2O_4$ + CuO.

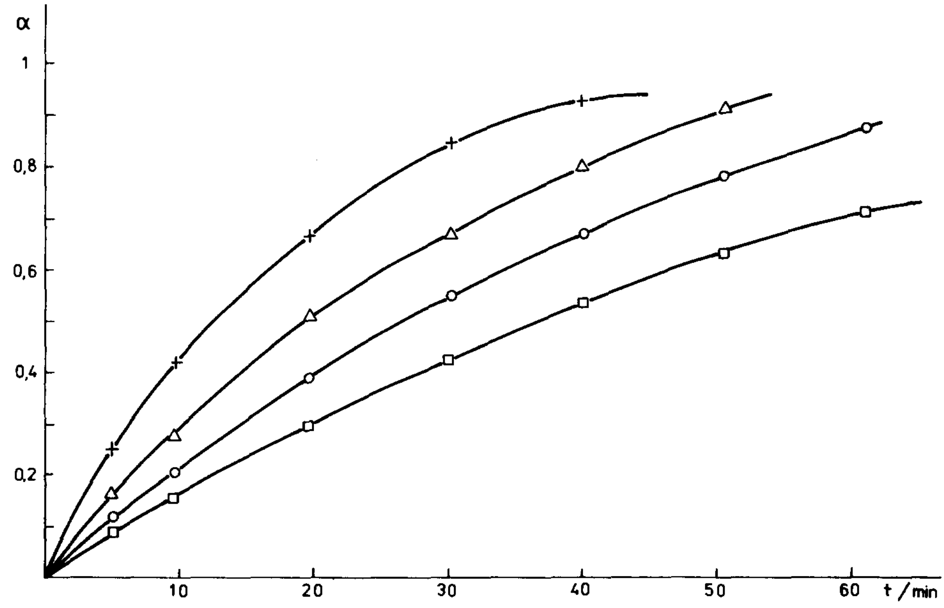

FIG. 9. The plot of α vs *t* for isothermal decomposition of $CuCrO_4$ in air at 753 K (□), 760 K (○), 767 K (△), and 773 K (+) examined by high-temperature X-ray diffraction.

An attempt to elucidate the reaction mechanism of thermal decomposition of $CuCrO_4$ (reaction (3)) with help of the high-temperature X-ray powder diffraction analysis led to different conclusions. The reason is that the decay of crystalline $CuCrO_4$ is a process proceeding in the first stage through an intermediate amorphous phase. In this stage, chains of CrO_4 tetrahedra and CuO_6 octahedra break down, to be adjusted for subsequent rate-determining second stage in which phase decomposition and reduction of the oxidation state of chromium take place. The formation of amorphous form of $CuCrO_4$ is manifested through increasing disperse halo in the angular interval 16–20° θ in the high-temperature powder diffraction diagram.

The results of X-ray analysis at temperatures 753, 760, 767, and 773 K in air are shown in Fig. 9. Transformation of α-curves from the type $\alpha = f(t)$ into the form $\alpha = f(t/t_{0.5})$ gives a distribution of the experimental points along a common curve, the shape of which can be approximated by the model reactions $F_1(\alpha) = -\ln(1 - \alpha)$ (first-order reaction) or $R_3(\alpha) = 1 - (1 - \alpha)^{1/3}$ (phase-boundary-controlled reaction with contracting interface). Evaluation of the rate constants and calculation of the activation energy from the temperature coefficients of the rate constants were based on the more probable kinetic equation $F_1(\alpha)$. The representative plots $\ln(1 - \alpha)$ vs t at different temperature levels are essentially linear (Fig. 10). A representative Arrhenius plot is shown in Fig. 11. The corresponding activation energy E_A for transformation of

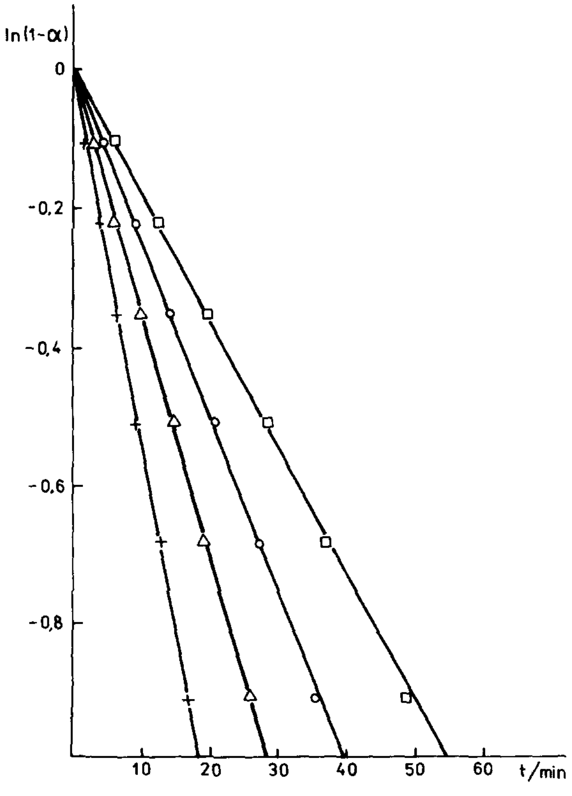

FIG. 10. The representative plot of the isothermal conversions in air by equation $\ln(1 - \alpha)$. The designation of temperatures is the same as in Fig. 9.

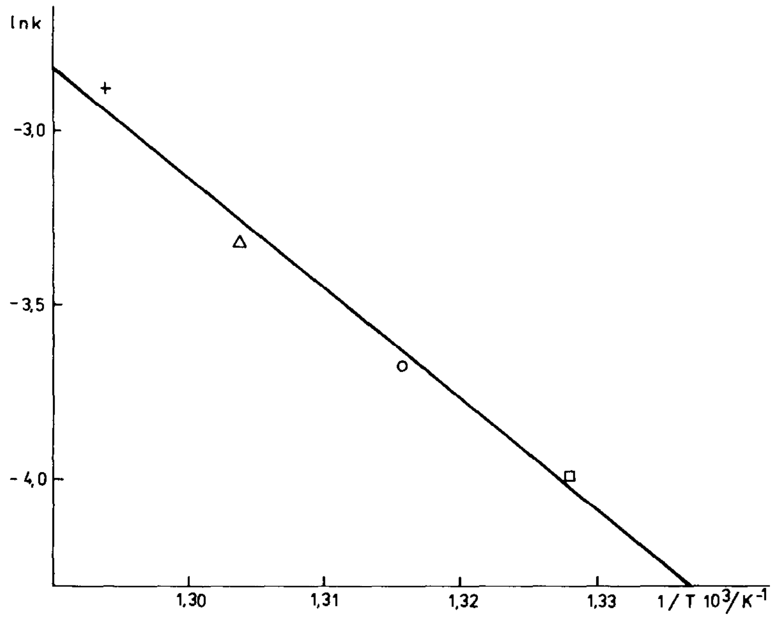

FIG. 11. The representative Arrhenius plot for thermal decomposition of $CuCrO_4$ in air examined by X-ray diffraction.

crystalline $CuCrO_4$ into amorphous form in air is 262 ± 4 kJ mole^{-1}. This value differs insignificantly from the activation energy E_A of decomposition reaction (3) governed through $A_2(\alpha)$ mechanism (248 ± 8 kJ mole^{-1}).

The catalytic activity and crystal imperfections arise, to our opinion, from the presence of Jahn–Teller active Cu^{2+} ions on the tetrahedral sites of the spinel-like structure of $CuCr_2O_4$ due to the strong preference of Cr^{3+} ions for the octahedral sites. This effect was first predicted by Dunitz and Orgel in their classical work (*19*). The compressed tetragonal distortion strains of the spinel-like structure cause also thermal instability of $CuCr_2O_4$ above 1173 K when dissociation reaction (2) takes place.

References

1. H. ADKINS, AND R. CONNOR, *J. Amer. Chem. Soc.* **53**, 1091 (1931).

2. H. ADKINS, E. E. BURGOYNE, AND H. J. SCHNEIDER, *J. Amer. Chem. Soc.* **72**, 2626 (1950).

3. J. D. STROUPE, *J. Amer. Chem. Soc.* **71**, 569 (1949).

4. A. IIMURA, Y. INOUE, AND I. YASUMORI, *Bull. Chem. Soc. Jpn.* **56**, 2203 (1983).

5. M. STAMMLER AND M. PYZYNA, *Adv. X-Ray Anal.* **7**, 229 (1964).

6. L. WALTER-LÉVY AND M. GOREAUD, *Bull. Soc. Chim. Fr.*, 830 (1973).

7. B. G. ERENBURG, V. P. FATEYEVA, A. I. MINKOV, L. M. SHADRINA, AND E. S. STOYANOV, *Izv. Sib. Otd. Akad. Nauk SSSR, Ser. Khim. Nauk* No. 4, vyp. 2, 54 (1981).

8. M. S. KOSNYREVA, A. I. PURTOV, I. I. KALINITCHENKO, AND D. M. DOROFEYEVA, *Zh. Prikl. Khim.* (*Leningrad*) **46**, 2515 (1976).

9. H. KITTEL, *Z. Anorg. Allg. Chem.* **222**, 1 (1935).

10. H. CHARCOSSET, P. TURLIER, AND Y. TRAMBOUZE, *C. R. Hebd. Seances Acad. Sci.* **254**, 2990 (1962).

11. P. PATANAIK, D. Y. RAO, AND P. GANGULI, *Thermochim. Acta* **68**, 17 (1983).

12. M. AVRAMI, *J. Chem. Phys.* **7**, 1103 (1939); **8**, 212 (1940); **9**, 177 (1941).

13. B. V. JEROFE'EV, *Dokl. Akad. Nauk SSSR* **52**, 511 (1946).

14. J. H. SHARP, G. W. BRINDLEY, AND B. N. NARA-

HARI ARCHAR, *J. Amer. Ceram. Soc.* **49,** 379 (1966).

15. C. H. BAMFORD AND C. F. H. TIPPER, "Reactions in the Solid State," Elsevier, Amsterdam/Oxford/ New York (1980).

16. R. G. DARRIE, W. P. DOYLE, AND I. KIRKPATRICK, *J. Inorg. Nucl. Chem.* **29,** 979 (1967).

17. G. PANNETIER, P. COURTINE, AND C. PERRAUDIN, *Bull. Soc. Chim. Fr.*, 3218 (1965).

18. K. BRANDT, *Ark. Kemi Mineral. Geol. 17A,* 1 (1943).

19. J. D. DUNITZ AND L. E. ORGEL, *J. Phys. Chem. Solids* **3,** 318 (1957).